

# Calibrating Point Spread Function for Motion Occlusion and Turbidity Removal in Underwater Imaging

Deepali N. Pande<sup>1</sup>, Satyajit Uparkar<sup>2</sup> and Kaushik Roy<sup>3</sup>

<sup>1-3</sup>Shri Ramdeobaba College of Engineering and Management, Nagpur, Department of Computer Application, Nagpur, India.

Email: pandedn@rknec.edu, uparkarss@rknec.edu, roykr@rknec.edu

**Abstract**—Underwater imaging over a dynamic water surface suffers from circular distortions prevalent in the fluid flow. We address the problem of motion let degradation during image formation in underwater dynamic refractive medium, experimented on swim art marshalling motion lets. We inspect the causes of motion distortion prominent through water turbulence, cyclic ripples in unidirectional water flow and refraction of light during imaging as light rays pass through air-fluid surface. The primary objective taken as a research outpost is finding appropriate technique to estimate point spread function of degraded framelets in underwater imaging. In evaluation of point spread function of degraded image, we have formulated an underwater image degradation model to measure motion blur on the basis of Jaffe-McGlamery theory, first accomplished in the UNCLES (Underwater Camera Light Experimentation System) imaging system. To measure the blur kernel, we designed a novel point spread function estimation algorithm compatible to the Jaffe-McGlamery underwater imaging system as a part of theoretical and experimental findings.

**Index Terms**— Image degradation, motion blur, Point Spread Function, Scale invariant Feature Transform, Underwater.

## I. INTRODUCTION

A driving challenge in the field of underwater (UW) imaging is to enhance and restore the quality of image. The underwater images suffer from various kind of degradation in which blurring is one of the most prominent one. One of the devastating problems in UW imaging is the limit of visibility during image acquisition through dynamic water surface, which has been the real platform of research [1]. Despite of the vivid applications of UW imaging, like fishery and marine engineering, one of the key applications is underwater diving training for coral reef management and many more. Water Borne imagery consists of multispectral images severely blurred due defocus between camera and the moving object [2]. In this scenario, estimation of the blur function and calibrating the level of degradation in motion blur images is a difficult task. There are several mathematical models available in the literatures which do not describe the parameters causal for degradation due to motion blur<sup>4</sup>. The motion blur degrades the original image in various aspects. The state-of-art techniques do not describe mathematical foundation needful to model the

type of motion blur. Under water imagery is one of the most important field of science needful in Olympic Games. Swimming has a former most out-front in Olympics [3]. In current systems, swimmers are trained using swim marshalling and swim finalizing training videos [7]. It is therefore useful to ascertain the quality of image needful to determine patterns of stroke propulsive forces during marshalling a swim trainee. Biomechanical biofeedback systems are commonly used in video recording systems for swim art marshalling which have terminal feedbacks. These systems are used to record the training episode during a swim art finalization with their feature of tactile modality. The trainee can later rewind to a certain motion clip and visually analyze each faux pas training sequence. They play a major role in motion tracking systems in form of markers to track biomechanical movement trajectories. The hardware composition of biomechanical feedback systems are basically, inertial sensors with MEMS (Micro electro mechanical systems) technology. The inertial sensors are used as one of the most contemporary technologies to augment a struggling performance in swimming. They combat the, formerly used faux pas video analysis systems traditionally used in biomechanical swim art marshalling. But these systems consume too much computational effort and lack quantitative information needful to edify the learner. Due to these shortcomings, the video analysis systems were gradually replaced with inertial sensors, fusion sensors and biomechanical motion sensors. A moving image is a 3D repository of useful information. But due to imperfect imaging systems, the recorded image is degraded invariably. A huge ratio of distortion results in uncertainty of the information contained. Restoring the original image from the degraded version requires finding the type of degradation. It requires forming a deblur kernel to restore the degraded image sampled from the spatially discrete image. The resultant imperfection in the imaging process can cause geometrical degradation or illumination imperfection amongst which, the former causes deviation in information content of the image. In this paper, the major focus is on analysis of motion deblur methods for forensics in swim art marshalling, biomechanical feedback system. We present inspection of motion blur induced during video imaging from biomechanical inertial sensors and present an analysis of motion Deblurring and reconstruction of original scene. A detailed inspection of MEMS (micro electromagnetic sensors) inertial sensors with varied range of accelerometer and gyroscope is presented using synthetic swim marshalling dataset and real world data retrieved using raspberry kit.

The paper is organized into four sections. In the literature review section, we present an in depth survey of point spread function estimation techniques and their state-of-the-art. In the mathematical formulation section, we present a mathematical base in modelling underwater image degradation. In this section, we frame the complete mathematical aspect of image degradation modelling and blur kernel estimation in underwater image degradation model and henceforth propose our research out-front in motion occlusion removal. We lay our experimental setup in the methodology section, using contemporary known algorithms to find, compute and approximate the point spread function over real world swim-art marshalling framelets and synthetically blurred images using renowned Cepstral transform and radon transform method. We also try and compare statistics of linear least square, Gaussian polynomial, hermite polynomial and Gaussian-hermite polynomial in PSF kernel approximation phase and depict the results of evaluation. We also present our PSF estimation algorithm implemented in java as a part of estimation.

## II. LITERATURE REVIEW

Image blur is identified as an unsharp image area. It occurs due to movement of subject in hitherto plane during imaging process. The inaccuracy in focusing of an aperture gives shallow depth of field. Identification of blur is very crucial in image restoration [1]. When the camera lens refocuses, conventional blur occurs in images due to out of focus, causing difficulty in identification of motion blur. To measure deskew, a method is proposed in [4] for estimating out of focus blur parameters robustly by using circular Hough transform and statistical measures that are based on mathematical modelling of zero crossing in log of Fourier spectrum, suitable only on ambient atmospheric conditions but incompetent in presence of dense refraction media. Authors in [3] present estimating the parameters of a motion blur like direction and length directly from the observed image with and without the influence of Gaussian noise and improve a given image in some predefined sense. The schemata poses incompetency when dealt with deblurring of motion lets from underwater imaging. Motion blur is a very common type of degradation caused by relative motion between subject and camera lens [4]. It can be modelled by a point spread function having two parameters angle and length. These parameters are essential for blind restoration of motion blurred images, accurately estimating these parameters are essential. These estimated parameters for motion blur are later used in a standard non-

blind convolution algorithm. Myriad researches in the field of blur deconvolution prove insufficient in blur kernel mapping in typical cases of motion frames caught in high contrast water turbidity and rigid deviation of white light in refraction phenomenon. Yet another novel approach to HDR (high-dynamic-range) image fusion [5] copes with image blur degradation existing in long exposed images. In this proposed approach, both camera and object motion blur are dealt in a computationally efficient manner which is also suitable for implementation on mobility and fog as the atmospheric conditions. In wireless sensor network short-exposed images are mainly affected by sensor noise than by motion blur, whereas longer exposed images are less noisy but significantly blurry. Using HDR fusion approach, the sharpness of short-exposed image and the noise-free characteristics of the HDR-fused image is retained by exploiting the differences between the image degradations. Hence, it can resolve both local and global blur caused due to object or camera motion. The problem of motion blur is quite complicated & difficult to resolve because of space variant, non-linear, and local characteristics. The information about motion if can be retained, then based on this motion may be recovered from blurred images. The authors in [6] have proposed an algorithm to recover motion blindly from a single motion-blurred image. A major contribution in this field lies in finding elegant motion blur constraint which is basically a linear constraint and it applies locally to pixels in the image. Hence, estimating global affine motion blur, global rotational motion blur, non parametric motion blur field estimating and segmenting multiple motion blur has been possible. The authors in [8] undertook the study of restoration of motion blurred images in spatial domain. They describe use of four types of techniques of deblurring image, two filter techniques like-Wiener filter, regularized filter and two convolution algorithms like, Lucy Richardson convolution algorithm and blind convolution algorithm, but these methods fail to recover pixels captured in dense frequency water turbulence. The method initially recovers surface slope pixels then gradually patches the neighbourhood displacement. There exist variations in the pixel field when motion lets are imaged in underwater hence; the pixel displacement patching used above is inapplicable in a 3D motion distortion pixel field space. Motion occlusion induced in UW imaging is a 3D turbulence refraction blur, so the contemporary 2D deconvolution techniques cannot map the point spread function of the blur kernel, thus causing phase shift in the pixels. If the contemporary 2D techniques are utilized in 3D motion deblurring, then the deconvoluted motion let incurs a phase-angular shift in each frame causing significant loss of semantic information. The major shortcomings of the state-of art point spread function estimation techniques is that they lack enough parameters to calibrate turbidity in dense refraction and hence could not be used in exact estimation of motion blur in underwater imaging. The contemporary PSF measurement techniques only comply with air images. We hypothesize this as a quantitative calibration of 3D blur kernel and thus lay an experimental set-up to frame schemata in measurement of 3D parameters of UW motion blur kernel.

### III. MATHEMATICAL FORMULATION

#### A. Under Water Image Formation

The still image imaging systems use long-exposure photography with information recorded in 2D or 3D form. The underwater imaging process comparatively differs from the normal imaging system. The motion image obtained in underwater imaging is formed by the propagation of electromagnetic waves in isotropic homogeneous media. The light interacts with matter through attenuation and scattering. The index of attenuation purely depends upon the salinity factor of water. The refraction factor deviates more as the salinity index increases. Hence, the magnitude of attenuation is fully dependent on salinity index. Another important parameter, is scattering which accounts the divergence of light from straight line path. The principle source of illumination in under water imagery is realm of light. The wavelength of light depends on the order of diffraction and the index of refraction. The motion image is a linear superposition of forward scatter, backscatter and direct component. When the light enters the camera without inception of reflection from the object, a backscatter is formed. In similar context, when light scatters with a small angle, it is measurable through forward component. Mathematically, motion imaging is represented in equation-1, below. We portray the underwater imaging components in Figure 1(a). The idea of motion occlusion due water turbulence is pictorially presented in Figure 1(b). The dashed line represents the direct component, dashed lines represent forward components and dash-dotted lines represent backscatter components.

The figure 1(a) shows an image formation model in underwater imagery of Jaffe-McGlamery in the UNCLES (Underwater camera Light Experimentation System), imaging system, the first accomplished one. The model represents a linear superposition of three major components namely direct component, forward scatter and the backscatter. The direct component  $E_{direct}$  is the light reflected by the object directly. The

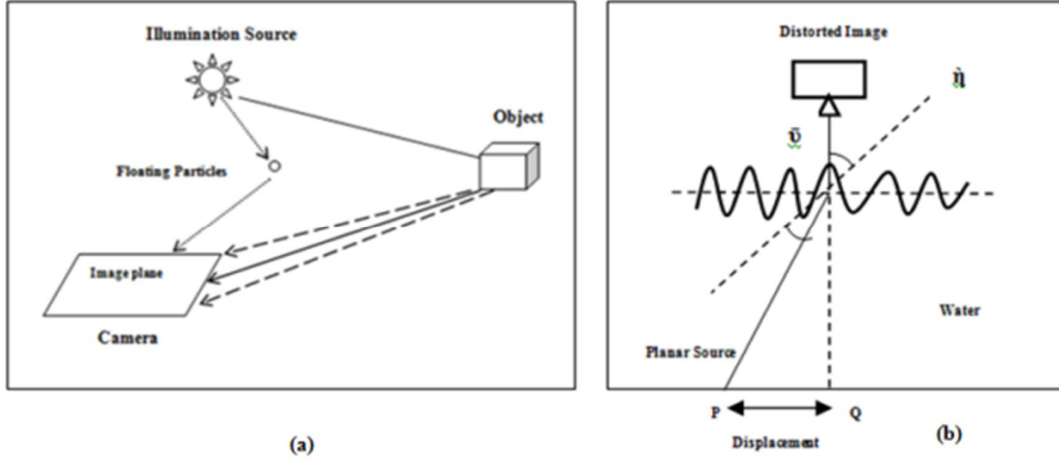


Fig. 1(a) illustrating Jaffe-McGlamery UW imaging Model first accomplished in the UNCLES imaging system. Fig. 1(b) is a Ray Defraction diagram picturing the occurrence of motion occlusion during UW imaging

$E_{\text{forwardscatter}}$  is the light reflected by the object at a scatter at a small angle and  $E_{\text{backscatter}}$  represents the light entering the camera due to floating particles. Hence the equation formed for total irradiance is given by,

$$E_{\text{total}} = E_{\text{direct}} + E_{\text{forwardscatter}} + E_{\text{backscatter}} \quad (1)$$

The physical properties of the medium cause degradation effect during the imaging process. Some of common factors affecting the degradation can be granulated as exponential attenuation of light during travel in water causing increased levels of turbidity. This results a direct impact of high values of forward scatter component and backward scatter component, the former causing significant blur and the later causing limited contrast levels. The absorption of light and the scattering of light path are causal due to presence of dissolved organic matter in water. Some of the additional factors are presence of floating particles and artificial light. We illustrated the underwater degradation process in Figure 1(b) using Ray diagram picturing degradation due refraction in presence of turbidity and floating components.

### B. Image Degradation in UW Imaging

#### Motion Vector Approximation

Identification of the source of motion blur is difficult problem. Myriad researches in this field show significant contributions in blur parameter estimations. The occurrence of motion blur in underwater imaging is most prominently due deviation in the illumination parameters like diffraction from the point of imaging and huge magnitude of refraction. The past researches in the field of underwater imagery depicts that the ambient light provides the illumination for imaging. Owing to these principles, we describe the motion blur approximation model considering the fact that illumination source takes a constant angular velocity corresponding to moving shutter. The motion scene lacks adaption to change of luminosity from frame to frame. We formulate this problem as,

$$F_1(x, y) = d(x - d_x, y - d_y) + w_1(x, y) \quad (1)$$

$$F_2(x, y) = d(x, y) + w_2(x, y) \quad (2)$$

Where  $F_1(x, y)$  and  $F_2(x, y)$  representation the motion frame with noise inception,  $d_x$  and  $d_y$  represent displacement components and  $w_1(x, y)$ ,  $w_2(x, y)$  are the Gaussian white noise components.

The real source of motion image degradation in under water imagery is induction of refraction and diffraction with a substantial ratio during the light tracing process from the illumination source. Most of the underwater imaging systems use range-gated systems to reduce the impact of backward scatter inception. To describe the motion image degradation model, we consider the image transmission in water as a linear system. The mathematical interpretation of motion image degradation is represented as,

$$g(x, y) = f(x, y) * h(x, y) + \eta(x, y) \quad (3)$$

Where  $g(x, y)$  is the observed image,  $f(x, y)$  is the original image,  $h(x, y)$  is the point spread function and  $\eta(x, y)$  shows the image is captured in presence of noise. The degradation function is convolved with the original image. The point spread function is an inception of turbidity in the medium response of imaging system. When practiced in frequency domain, the motion image degradation is represented as,

$$G(u, v) = F(u, v) H(u, v) + N(u, v) \quad (4)$$

Wherein the  $(u, v)$  represents spatial frequency and  $G, F, H, N$  are the Fourier transforms of  $g, f, h, n$ . We describe the optical transfer function and the modulation transfer function capability of  $H(u, v)$  as the degradation function in our Motion Image Degradation Model below.

Finding the real cause of degradation to estimate the point spread function is tedious and impractical in current forensics systems. There are several mathematical techniques but none commit to obtain the exact parameters of the PSF. In such scenarios, to obtain a correct estimate of degradation, an appropriate model of PSF from well known models has to be opted. To evaluate this, we present our experimental work in table-1. When a motion video is captured in underwater imagery, the object is imaged over a three dimensional (3D) object space projected onto  $P$  different positions  $(x_p, y_p)$  where  $p = 1: P$ , in a two dimensional image plane as illustrated in figure-1. We relate the image point with the object point using the homogeneous vectors as

$$[x_p, y_p, 1]^T = \Pi_p [X, Y, Z, 1]^T$$

Here  $\Pi_p$  represents the projection matrix of the  $p^{\text{th}}$  camera pose.

Assuming that the motion trajectory is generated invariant to the space, then the  $P$  points in the image plane generate the point spread function of the corresponding motion blur is represented as,

$$h(m, n) = \frac{1}{P} \sum_{p=1}^P \delta(m - x_p, n - y_p)$$

Hence, knowing the space-invariant PSF, the image degradation model of the motion blur is given in the vector-matrix form as,

$$g = Hf + \eta,$$

Where ‘ $g$ ’ represents the motion blurred image,  $H$  is the degradation matrix,  $f$  is the ideal image without motion blur, and  $\eta$  is additive noise. The scene points are projected onto the image plane according to the projection matrix by estimating the motion PSF.

#### *Blur Kernel Estimation in Underwater Image Degradation*

In this section, we are discussing Fourier Transform of Motion Blur angle estimation and Histograms of Oriented Gradients in that order for Motion Blur Length Estimation.

We stick to the basis that the occurrence of motion blur is due to the relative motion between camera and the object when the object is being captured. Working on the hypothesis that the blur occurs when the motion has constant speed and a fixed direction, we present the mathematical description of motion blur angle estimation using Fourier transform and then structuring it for finding Motion blur length using histograms of oriented gradient. We aim to construct the point spread function in estimation of the key parameters, the motion angle and the motion length to formulate the Deblurring algorithm.

In equation-3, the process of blurring is modeled where  $f(x, y)$  is the original image;  $h(x, y)$  is the blurring point spread function and  $\eta(x, y)$  is white noise and  $g(x, y)$  is the degraded image. Using this, we represent the point spread function for linear motion blur with length of  $L$  and angle  $\theta$  is given by

$$h(x, y) = \frac{1}{L} \delta(\vec{L}), \quad (5)$$

Here  $\vec{L}$  is the segment of length  $L$  is oriented at angle  $\theta$  degrees from the  $x$ -axis. Equation-4, represents the Fourier transform of the degradation function from which, neglecting noise we get,

$$G(u, v) = F(u, v) H(u, v) \quad (6)$$

To form an integral function, we consider the movement of the camera during time T in horizontal (x) and vertical (y) directions being x(t) and y(t), we obtain,

$$g(x, y) = \int_0^T f(x - x(t), y - y(t)) dt \quad (7)$$

Applying Fourier Transform to equation (7), yields,

$$\begin{aligned} G(u, v) &= \iint_{-\infty}^{\infty} \left[ \int_0^T f(x - x(t), y - y(t)) dt \right] e^{-j2\pi(ux+vy)} dx dy \\ &= \int_0^T \left[ \iint_{-\infty}^{\infty} f(x - x(t), y - y(t)) e^{-j2\pi(ux+vy)} dx dy \right] dt \\ &= F(u, v) \int_0^T e^{-j2\pi(ux+vy)} dt \end{aligned} \quad (8)$$

Hence, we get,

$$H(u, v) = \int_0^T e^{-j2\pi(ux+vy)} dt.$$

If the movement distance during T in the x and y directions are 'a' and 'b', respectively then x(t) = at/T and y(t) = bt/T which yields,

$$H(u, v) = \frac{T \sin(\pi(ua+vb))}{\pi(ua+vb)} e^{-j\pi(ua+vb)} \quad (9)$$

It can thus, be seen that when the quantities H(u,v) and G(u,v) equal to zero when  $\theta = s, 2s, \dots, ms$ . Hence, the log spectrum of the blurred image Logs(u,v) is described as,

$$\text{Log}(u, v) = \log(1 + |G(u, v)|) \quad (10)$$

#### *Measuring Blurred Image Spectrum in Underwater Turbulence*

**Hypothesis-** Theoretical understanding of underwater turbulence is not as developed as atmospheric turbulence. The caveat to use convolution is an inexact method to model Motion Blur & Turbulence. The deviation in luminance spectrum in trigonometric plane induces motion blur. The motion blurred image is the degradation caused by sampling in presence of irregular luminance spectrum. We aim to recognize the type of the motion blur caused due to luminance spectrum degradation and Kolmogorov turbulence in Underwater Imaging.

#### IV. PROBLEM STATEMENT

**Research Outfront-** There are no promising methods to calculate Point Spread Function (Transfer function) capable of accurately mapping the response of underwater imaging system in high proportion motion blurred motionlets. Hence, it is necessary to lay a proof of concept in the theoretical understanding of underwater turbulence & its suspension to cause motion blur. The development of information retrieval technique is highly complex as it requires finding spatial correspondences amongst each framelet in the scene images.

Image registration is the technique of transforming different sets of data to one coordinate system. To establish the relationship between the reference image and the degraded image, we perform image registration considering the fact that the incepted variations occur during the acquisition process. Since our major purpose is swim art marshalling, we aim at obtaining a blur free motion let from scene video to target photogrammetry followed by rotoscoping of the swim strokes. Keeping motion deblur as the basis step, our orientation is retrieving motion lets of swim strokes to stitch a swim art marshalling scene. The step of registration is opted since the motion videos are extracted from different sensors. The video has been captured at time-variant slots during the training exercise. The image registration process defines a mapping between two images both spatially and along with intensity. The mapping  $I_2(x, y) = g(I_1(f(x, y)))$  where 'f' is 2D affine transformation function mapping original spatial coordinates to new spatial coordinates,  $(x', y') = f(x, y)$ .

The affine transformation works on the basis that the property of the object remains intact during the process. The variations refer to the differences in the values and locations of pixels between two images which can be volumetric or radiometric. Image registration basically requires spatial transformation to precisely overlay

two framelets. Only an appropriate class of transformation can remove spatial distortions incepted during the acquisition process.

## V. METHODOLOGY

### A. Scale Invariant Feature Transform

We use Scale invariant feature transform algorithm to retrieve local feature descriptors of scene images. A range of reference images and key points are extracted from the scene motion. We extract SIFT key points and store each of them as a reference database. The Euclidean distance computation matrix of the reference image and the target image is computed to determine subsets of key points which agree on the test image as its location, scale and orientation. We describe the image registration process in the section below.

### B. Proposed 3D PSF Extraction & Regularization for Underwater Motion Distortion & Turbulence Factor Deconvolution

In our experiment, we examine different methods of 3D PSF kernel regularization by using statistical bases. We analyze the solution for kernel mapping to represent the intrinsic shape of the PSF matching kernel. The strength of regularization  $\lambda$  is set to allow some degrees of freedom depending on the kernel size. An overestimation in the size of kernel and degrees of freedom can in a pair can yield noisy kernel having large variance. We developed a Matlab program to obtain continuous trajectory curve on a pixel grid using sub pixel linear interpolation. The algorithm for performing interpolation and PSF generation is illustrated below. It is validated in Matlab2011a and developed in Java using standard image processing libraries. It successfully estimates the speckle transfer function for deducing Kolmogorov underwater turbulence and its hitch to cause motion blur.

PSFs are obtained by sampling the continuous trajectory Traj\_Curve on a regular pixel grid using linear interpolation at sub-pixel level. The input to the system is motion blur trajectory curve provided by Create\_Trajectory function, PSF\_size is size of the PFS where the TrajCurve is sampled, and 'T' is a Vector of exposure times for each PSF generated, while output is store using do\_center, PSF\_Sample cell array containing PSF\_Sample sampling TrajCurve for each exposure time in T.

---

#### PSF Sampling Algorithm

---

1. Extract the values of Trajectory Curve by computing trajectory, size of PSF, and exposure time T.
  2. Calculate the length of exposure time and store in 'T' and store invariable PSF number.
  3. Compute the samples of motion trajectory.
  4. Calculate the centre with respect to baricenter using,
 
$$x = x - \text{mean}(x) + (\text{PSF\_size}(2) + 1i * \text{PSF\_size}(1) + 1 + 1i) / 2;$$
  5. Generate PSF samples using,
 

```
PSF_sample = cell(1, PSF_number);
PSF = zeros(PSF_size);
triangle_function = (d) * max(0, (1 - abs(d)));
triangle_fun_prod = (d1, d2) * triangle_function(d1) * triangle_function(d2);
```
  6. Set the exposure time previous\_T = T(j - 1)
  7. Sample the trajectory until time T
 

```
for t = 1: numel(x);
    if (T(j) * numt >= t) && (prevT * numt < t - 1);
        t_proportion = 1;
    elseif (T(j) * numt >= t - 1) && (prevT * numt < t - 1);
        t_proportion = (T(j) * numt) - (t - 1);
    elseif (T(j) * numt >= t) && (prevT * numt < t);
        t_proportion = t - (prevT * numt);
    elseif (T(j) * numt >= t - 1) && (prevT * numt < t);
        t_proportion = (T(j) - prevT) * numt;
```
-

```

else
    t_proportion = 0;
end
    m2 = min (PSF_size (2)-1, max (1, floor (real(x (t)))));
    M2 = m2+1;
    m1 = min (PSF_size (1)-1, max (1, floor (image(x (t)))));
    M1 = m1+1;
8. Compute linear interpolation using, for all quadrants,
   Compute PSF(m1 , m2) = PSF(m1 , m2) + t_proportion * triangle_fun_prod( real(x(t)) - m2 ,
   image(x(t)) - m1 );
9. Perform PSF normalization.

```

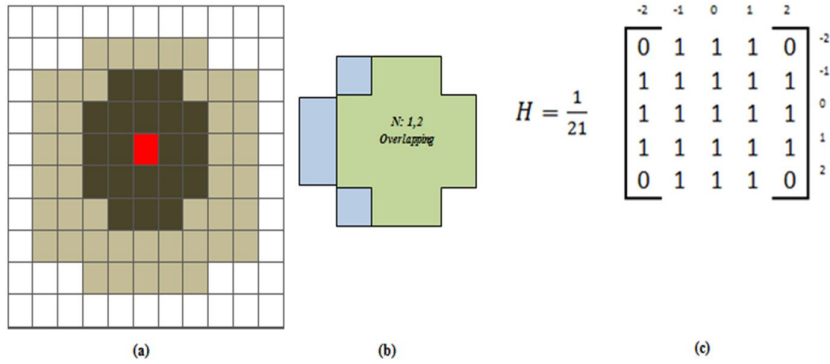


Figure 2. A pixel grid with a neighborhood of pixels with two overlapping neighborhoods is shown. It is a union of 21 neighborhoods with the red pixel in the centre as the intersection of neighborhoods. A kernel with diameter 5 pixels is used for approximation

The Point Spread function generation algorithm is performed in Matlab 2011a using Intel core i3 processor and 4 GB RAM with 2.4 GHZ capacity. We need to first compute the trajectory for inter-linking all the frames in the video. The motion kernel PSF differs for each frame in the video. Hence, we need to evaluate the PSF of each frame and perform interpolation in space co-ordinates. Doing this, we get a complete PSF kernel estimation with individual kernels stitched together. This gives a broader view of the actual motion occlusion in consideration of the framelets as a whole.

The figure-2 represents a theoretic neighborhood view of pixels on the pixel grid to approximate the blur circle of diameter 5, as a customization to our PSF Algorithm. The two pictures in figure-2 show two overlapping neighborhoods with a union of 21 neighborhoods comprising at the centre of red pixel. In such a scenario, we define a 5 X 5 matrix point spread function having neighborhood of 21 pixels, 1/21 having all pixels a value one except the corner ones which will have value zero. In doing this, the PSF function H matrix is defined as shown in Figure (c).

In our experimental set-up we perform PSF estimation on synthetic motion blur and sensor retrieved motion blur framelets using varying kernel sizes and accordingly approximates the values of degrees of freedom and the strength of regularization. The values taken during the experimental phase is illustrated in table I.

TABLE I. PSF APPROXIMATION IN UNDERWATER TURBULENCE MOTION LETS

Kernel Size	Statistical Base	Degrees of Freedom	Strength of Regularization $\lambda$
17 X 17	Linear Least Square	180	$\lambda = 1.0$
19 X 19	Gaussian Polynomial	260	$\lambda = 5.0$
21 X 21	Hermite Polynomial	361	$\lambda = 7.0$
51 X 51	Gaussian-Hermite	361	$\lambda = 10.0$

Let the image matrix be represented as  $I(m, n)$  and Kernel function as  $H(u, v)$  then deconvolution using the point spread function will be computed iteratively using a classic approach as,

$$I_{\text{deblur}}(r, c) = \sum_{u=-2}^2 \sum_{v=-2}^2 H(u, v) I(r - u, c - v)$$

### C. Motion Deblurring in Underwater Media

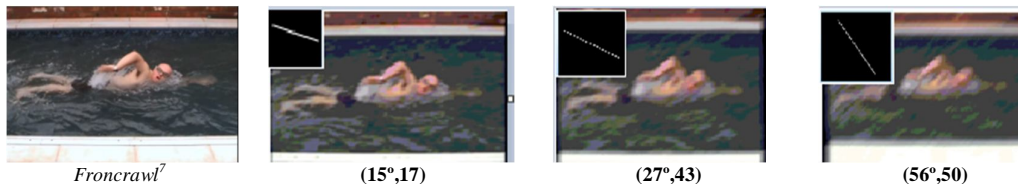
Spatial deblurring requires that the blur kernel is shift-invariant. But underwater motion blur could not use spatial deblurring technique, as it is highly complicated to deconvolve it on frame-by-frame basis as compared to atmospheric blur. It is a real area of research to deblur motion of a single frame from scene containing motion occlusions in UW imaging scenario. We perform analysis over myriad approaches to deconvolve the distortions in the motion scene and try estimation of the best-match PSF in the described scenario. We depict estimation of the key components in motion deblurring namely the motion blur angle and the motion blur length using contemporary methods in the table 2 below applied on underwater imaging.

TABLE II. SIMULATION VALUES IN BLUR ANGLE AND BLUR LENGTH ESTIMATION. LENGTH VARIATIONS 20 PIXELS IN PRESENCE OF 35 DB NOISE LEVEL

Estimation	UW Motion Blur Angle $\theta^\circ$		UW Motion Blur Length L (in pixels)	
	Cepstral Transform	Radon Transform	Cepstral Transform	Radon Transform
Best Estimate	0	0	1	1
Worst Estimate	2.14	2.18	6	6
RMSE	0.7734	0.8733	1.446	2.7654
NRMSE	0.0.899	0.0413	0.0557	0.0978

## VI. EXPERIMENTS & RESULTS

The Matlab implementation of the method took 254 seconds to estimate the motion kernel size of a 512 X 512 blurry image on a computer with an Intel core i3, 2 GHz processor. An in-detail evaluation of motion occlusion on real blur captured during imaging process is presented with three well known strategies, namely large kernel size 50 X 50, baseline moderate kernel size 21 X 21. We also evaluated the approach on synthetic blurs generated by producing motion blur with angular varying positive theta on 50 sharp images. We show the corresponding results in figure 3. Figure 3(a) represents the framelets extracted during swim stroke retrieval from swim art marshalling underwater video imaging process, represents a clear image. Figure 3(b) is the underwater motion Turbulence Blur extracted using data retrieval process from TriAxyl sensor UW imaging system. The pictures used are the courtesy of Eastern Sports Association Swimming Club, India. In figure 3(b), the blur kernels are estimated with different  $\theta^\circ$  and length scale. The figures in second, third and fourth column illustrate estimated PSFs in varying timeframes of video framelets. We estimated the size of the kernel, using state-of-the-art statistical kernel estimation techniques and deblurring algorithms to estimate the actual motion kernel. We measured the estimated kernel size in terms of the Peak Signal-to-Noise Ratio (PSNR) and Structural Similarity (SSIM) as a metric. In Blur Kernel Estimation, to accurately find the blur kernel estimation we implemented the algorithm for calculating structural similarity index (SSIM) between two images. The SSIM is the image quality metric based on an image with high quality reference image. We used the SSIM for objective analysis of the synthetically blurred image. In our method, we used four different techniques in PSF estimation namely the Radon transform, the Fergus method, and two blind deconvolution methods, SJA's technique and Cho's fast blind deconvolution techniques.



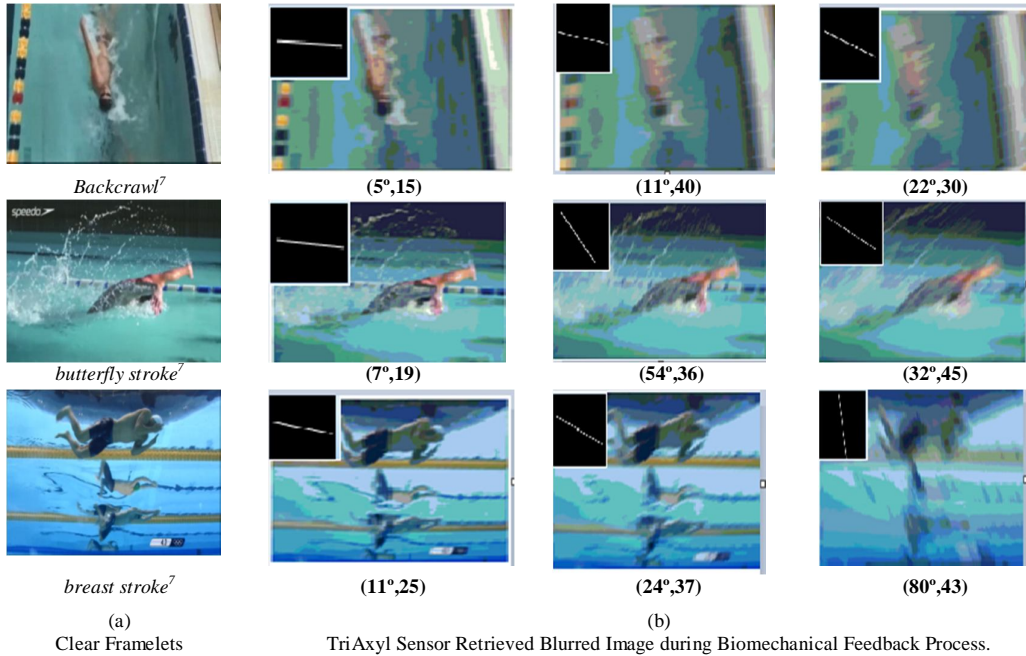


Figure 3(a). Illustration of Framelets representing different strokes in swimming. Figure 3(b) Illustration of PSF Extraction using Proposed Algorithm

**Figure 3(a)** are the framelets extracted during swim stroke retrieval from swim art marshalling underwater video imaging process, represents a clear image. **Figure 3(b)** is the underwater motion Turbulence Blur extracted using data retrieval process from TriAxyl sensor UW imaging system. The pictures used are the courtesy of Eastern Sports Association Swimming Club, India. In figure 3(b), the blur kernels are estimated with different  $\theta^0$  and length scale. The figures in second, third and fourth column illustrate estimated PSFs in varying timeframes of video framelets.

We used Logistic and Gaussian functional form of the kernel to blur the images synthetically with  $\lambda$ -max correlation coefficient. We illustrate this in figure 4 (a) & 4(b) which represent the interpolation of PSFs on framelets obtained during video imaging in (a). Figure in 4 (b) represent the data retrieval from sensor. The outputs of interpolation are stored in form of interpolation trajectory to estimate the ultimate framelets PSF in video imaging. In our PSF estimation experimental phase, we performed various edge detection algorithms on the synthetic blur image and compared it with the real blur image. To model the blur kernel estimation we comparatively used various edge detectors Sobel, Prewitt and Roberts and retrieved functional form, support size and variance from each test image. As with our hypothesis, there are boundaries beyond which the PSF estimation techniques can be optimized to determine the type of the blur.

## VII. PERFORMANCE ANALYSIS WITH STATE-OF-ART

The algorithm is computationally fast and it requires enough amount of operating memory to handle long image sequences. Owing to this, we have kept the size of the kernel as 17 X 17, 21 X 21 and 51 X 51 for combination of frame-lets. Our image degradation model illustrated luminance distortion due to turbidity, white light and refraction. Hence, we quantify Kolmogorov turbulence factor from it. The turbulence fluids are characterized by velocity and diameter of circular eddies. The number of grid points and baricenter necessarily accountable is proportional to  $R^{9/4}$ , where 'R' is the Reynolds's Number. Hence, the proposed Speckle Transfer function (Point Spread Function) computes baricenter of eddies fitting into combination of kernel sizes 17 X 17, 21 X 21 and 51 X 51. Deconvolution can be correctly done only of sufficient PSF value is obtained. In regard to this, it is noteworthy to precisely estimate the correct point spread function in underwater motion lets. To accelerate the results, we used 64 bit Windows 7, with 3.4 Ghz CPU and 8 GB Ram and iteratively solve to obtain accurate PSF. The proposed algorithm outperforms the contemporary bispectrum technique used in estimating optical transfer function. Instead of using thousand frames, the

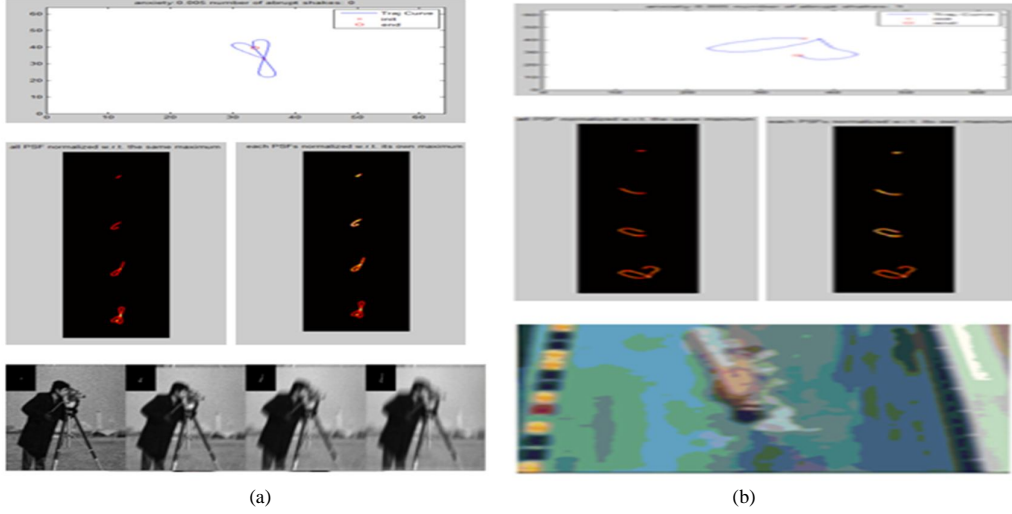


Figure 4 (a) & (b) illustrate interpolation of PSFs on framelets of video on recording in (a) and (b) sensor retrieved in (b). The outputs of interpolation are stored in form of interpolation trajectory to estimate the ultimate framelets PSF in video imaging

proposed method works even in hundred frames per evaluation. When conducted a Peak signal to noise ratio and root mean squared error, our method shows 95 percent accuracy over 50 framelets in consideration. We illustrate the convergence inspection in table 3 below, respectively performed on two real life datasets obtained from Eastern Sports Club.

TABLE III. CONVERGENCE TEST ON THE PROPOSED PSF EXTRACTION ALGORITHM IN METHODOLOGY STEP-2

	<i>Dataset-1</i>	<i>Dataset-2</i>
Iterations 'k'	22	27
Computation time ' $\mu$ '	184.55 seconds	198.76 seconds
$\alpha_{ROC}$ Rate of Convergence	4.7	7.3
Number of Framelets	50	55

Our method was compared to analyze the results from a set of 50 PSF realizations each for noise conditions ranging generated at range  $t_s = 2\mu m$ . The image space taken into consideration is  $51 \times 51$ . To test its convergence, we used noise-filtered motion lets thoroughly passed through rate of convergence (ROC) given by [20],

$$\alpha_{ROC} = \frac{\log \frac{e^{(m+1)}}{e^{(m)}}}{\log \frac{e^{(m)}}{e^{(m-1)}}}$$

Here  $e(m) = t_s^{(m)} - t_s^{(m-1)}$

The convergence criterion used for analyzing the estimation method was based on surrogate and paraboloidal function in 3D trigonometric plane to assess eddies in turbidity saturated condition. We considered success percentage for comparing the number of iterations falling in the interval of initial estimates.

## VIII. DISCUSSION & CONCLUSION

We studied and evaluated camera motion deblurring techniques as propounded in the literature. During the initial test with the underwater imagery motion blurred images, we determine that the edge profile methods show low performance in convergence of deblur procedure. We also studied in the experimental phase that the complex kernels in the motion blur of camera sensor imagery have non-analytic shapes and are hard to converge to kernel estimation statistics due inherent dissymmetry in motion blur frame-lets. Hence, it is possible to use fast edge profile PSF estimation to correctly opt the initial guess and the baricenter in the

kernel approach. During our experimental study, we noticed that it is difficult to differentiate between edge profiles in presence of high proportion of noise, but still the contemporary methods show satisfactory results in point spread function estimation and hence deconvolution. The scene retrieval algorithms are in development which we will present in the next phase. The point spread function estimation algorithm proposed outperforms the contemporary methods in motion blur estimation and blur kernel formation aiding to simplify and fasten the motion deblurring process. We portrayed the Jaffe-McGlamery UW Imaging model to produce the Underwater Image Degradation for motion blur and evaluated its blur kernel using contemporary kernel estimation techniques. During the experimental test, it was observed that the phase shift angular displacement factor is needful for formulating a motion deblur algorithm. To measure the blur kernel, we designed a novel point spread estimation algorithm compatible to the Jaffe-McGlamery underwater imaging model. During the initial test with the underwater imagery motion blurred images, we compared our PSF algorithm with contemporary methods and studied that the edge profiles methods show low performance in convergence of deblur procedure. We also studied in the experimental phase that the complex kernels in the motion blur of camera sensor imagery have non-analytic shapes and are hard to converge to kernel estimation statistics due inherent dissymmetry in motion blur frame-lets. Hence, it is possible to use fast edge profile PSF estimation to correctly opt the initial guess and the baricenter in the kernel approach. In future, we are aiming to retrieve swimming strokes for designing a swim art training & marshalling kit.

#### REFERENCES

- [1] S. Naeth, D. Shumuk, and T. Ethier, "TRIAXYs g3 Directional Wave Sensor Latest Developments for Next Generation Wave Sensor Technology 2016", OCEANS 2016 MTS/IEEE Monterey, CA, USA. 19-23 September 2016.
- [2] J. Magnetic and J. Marshall, "Magnetic Field Swimmer Positioning", IEEE Sensors Journal. Vol. 15(1). pp. 172–179, 2015. ISSN: 1530-437X.
- [3] N. Kaur and N. Mahajan, "Image Forgery Detection using SIFT and PCA Classifiers for Panchromatic Images", Indian Journal of Science and Technology. Vol. 9. Issue No 35. 2016 Jun; 9(21):1–8
- [4] S.Tiwari, V. P. Shukla, and A. K. Singh, "Review of Motion Blur Estimation Techniques", Journal of image and Graphics. Vol. 1, No. 4. pp. 176–184, 2013.
- [5] [www.academia.edu/6880139/Review\\_of\\_Motion\\_Blur\\_Estimation\\_Techniques.pdf](http://www.academia.edu/6880139/Review_of_Motion_Blur_Estimation_Techniques.pdf)
- [6] Natasha Gelfand, Kari Pulli, Marius Tico, "Motion-Blur-Free Exposure Fusion" Proceedings of 2010 IEEE 17th International Conference on Image Processing H. Kong, pp. 3321–3324, 2010.
- [7] S. S. Al-amri, "A Survey on Various Image Deblurring Methods", International Journal of Computer Science and Technology. Vol. 4. No-3.PP-168-172.
- [8] S. H. Chan, S. Member, and T. Q. Nguyen, "LCD Motion Blur : Modeling, Analysis, and Algorithm", Journal of Transactions on Image Processing. Vol. 20, No. 8. pp. 2352–2365, 2011.
- [9] Z.Y. Wen, D. Fraser, H.D. Li, "Reconstruction Of Underwater Image By Bispectrum" in proceedings ICIP 200, pp 545-548.
- [10] C. Matson, "Weighted-least-squares phase reconstruction from the bispectrum," J.Opt.Soc.Am.A, Vol. 8, pp. 1905–1913, 1991.
- [11] D. Kundur, D. Hatzinakos, "Blind image deconvolution", IEEE Signal Processing Magnetics, Vol. 13, No. 3, pp. 43-64, 1996.
- [12] 2.C. Yu, C. Zhang, L. Xie, "A blind deconvolution approach to ultrasound imaging", IEEE Trans. Ultra son. Ferroelectric. Freq. Control, Vol. 59, No. 2, pp. 271-280, 2012.
- [13] G. Dougherty, Z. Kawaf, "The point spread function revisited: Image restoration using 2-D deconvolution", Radiography, Vol. 7, No. 4, pp. 255-262, 2001.
- [14] N. Dey, L. Blanc-Feraud, C. Zimmer, P. Roux, Z. Kam, J.-C. Olivo- Marin, J. Zerubia, "Richardson-Lucy algorithm with Total Variation Regularization for 3D Confocal Microscope Deconvolution", Microsc. Res. Tech, Vol. 69, No. 4, pp. 260-266, 2006.
- [15] Christoph Dalitz ;Regina Pohle-Frohlich ;Thorsten Michalk, "Point Spread Functions and Deconvolution of Ultrasonic Images", IEEE Transactions Ultrasonic, Vol. 62, Issue 3, pp. 531-544.